Numerical Investigation of Secondary Flow In An Axial Flow Compressor Cascade

[1]T. Suthakar, [2]Akash Dhurandhar
[1]Associate Professor, [2]M.Tech. Scholar,
Department of Mechanical Engineering
National Institute of Technology, Tiruchirappalli – 620015
Tamil Nadu, India

Abstract
A numerical study has been conducted for steady, three dimensional viscous flow fields in an axial flow compressor cascade focusing basically on the secondary flow formation. The study is made on the basis of static pressure distribution along the blades with different inflow angles. The k-ε model was used and a finite volume method was employed to solve the flow governing equations. The present work consists of a compressor cascade analysis with chord length of 5 units and pitch of 0.55 times chord length. For this analysis ideal gas is taken as the fluid with atmospheric pressure and a temperature of 300 K, $\alpha_i = 26.5^o$, 35^o and 45^o, Ma = 0.66, Re = 0.6 x 10^6. Flow analysis is carried out using commercial CFD codes (Fluent 6.3.26). The computational results support the secondary flow occurrence in a compressor cascade for specific conditions.

Key words: secondary flow, turbulence intensity, axial compressor cascade, cascade losses

Nomenclature

Re	Reynolds number
Ma	Mach number
S	Cascade pitch
C	Chord
h	Blade height
Cp	Pressure coefficient

Greek letters

α_i	inlet air angle
α_e	exit air angle
θ	stagger angle

Introduction
Accurate prediction of turbo machine cascade flow and pressure losses remains a challenging task despite a lot of work in this area [4]. Flow in a cascade of turbo machinery suffers various types of losses like annular loss, profile loss and last but not the least secondary losses. The term secondary flows refers to the three- dimensional vortical flow structures that develop in blade passages due to high turning of the flow and non uniform inlet total pressure profiles. [2]. Flow which is transverse to the primary flow direction is termed as secondary flow [2]. Secondary flows are important source of losses in turbo machines, especially in cascades with short height blading and high flow turning. The secondary flows originate from specifically developing end wall boundary layers and are associated with the presence of longitudinal vortices with a dominant stream wise component of the vorticity. They are driven by transverse static pressure gradients and mass forces acting on fluid elements in curvilinear motion through the blade passage. The secondary flows also modify the shape of end wall boundary layers from which they originate [9].

In compressors the classical secondary flow is not so strong because the blade turning is low. However, the end-wall boundary layers are thick and are prone to separate in the corner between the suction surface and the end-wall. This separation is greatly influenced by both secondary flows, which tend to exacerbate it, and tip leakage flows, which tend to prevent separation [6]. The main type of secondary flow is the induced recirculating flow, which leads to the formation of a passage vortex. The source of the induced recirculating flow is the cross flow in the end wall boundary layer that forms as a result of force equilibrium in curvilinear motion.

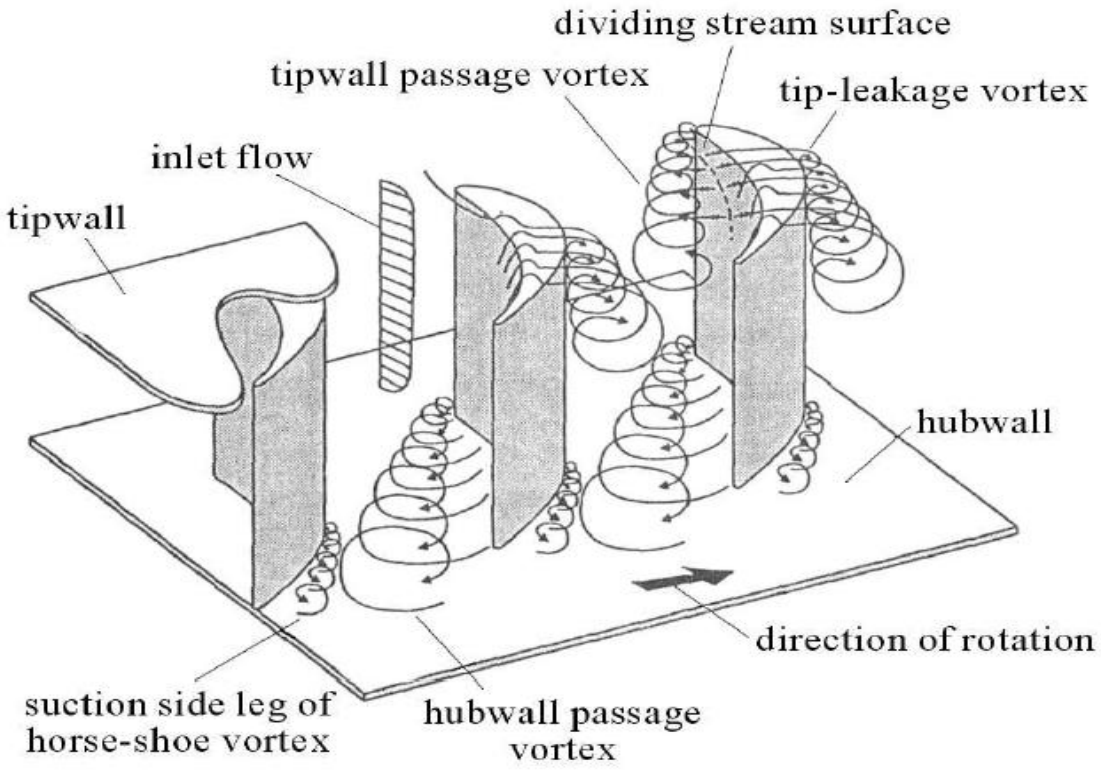

Figure 1: Various types of secondary flows in a cascade of turbo machine.

Mechanisms of secondary flow

Within a blade passage in a cascade, a deflection of the low momentum fluid equal to the mainstream deflection would not be sufficient to obtain the balance between the pressure gradients and the centrifugal forces. As a result the low momentum fluid turns more than the mainstream flow and this deviation from a uniformly deflected stream called secondary flow [11].

The term secondary flows refers to the three-dimensional vortical flow structures that develop in blade passages due to high turning of the flow and non-uniform inlet total pressure profiles. The boundary layer flow along the end wall contains span wise velocity gradients. When the boundary layer flow is turned, transverse velocity components are introduced. These secondary flows, created at the end wall and blade junction, extract energy from the fluid which would otherwise be used to rotate the blades or produce thrust [2].

The secondary flows originate from specifically developing end wall boundary layers and are associated with the presence of longitudinal vortices with a dominant stream wise component of the vorticity. They are driven by transverse static pressure gradients and mass forces acting on fluid elements in curvilinear motion through the blade-to-blade passage [9].

Methodology

Table 1 Details of Investigation

1	Aspect ratio, c/h	1
2	Chord length, c	5 units
3	Pitch of the cascade	0.55 c units
4	Inflow angle (in degree)	26.5 , 35 and 45
5	Mach No.	0.66
6	Reynolds No.	0.6 x 10^6
7	Viscous model used	k-epsilon
8	Software used	Gambit and Fluent
9	Type of analysis	3D

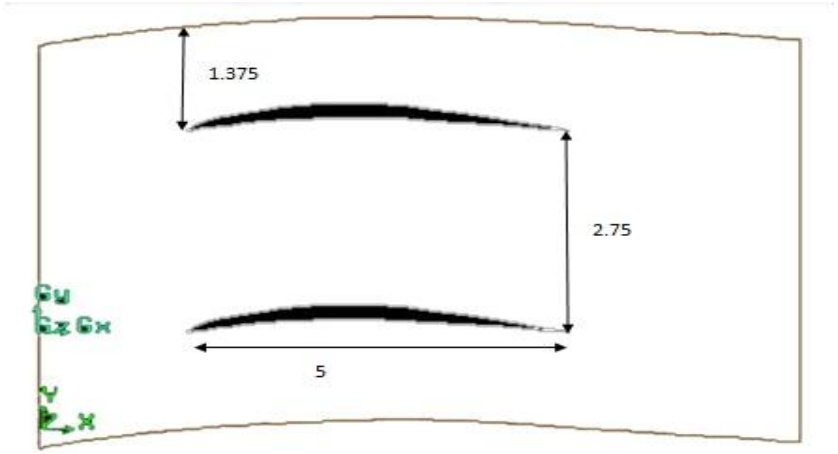

Figure 2: Dimensions of cascade

Using these dimensions three dimensional models are drawn out from this arrangement.

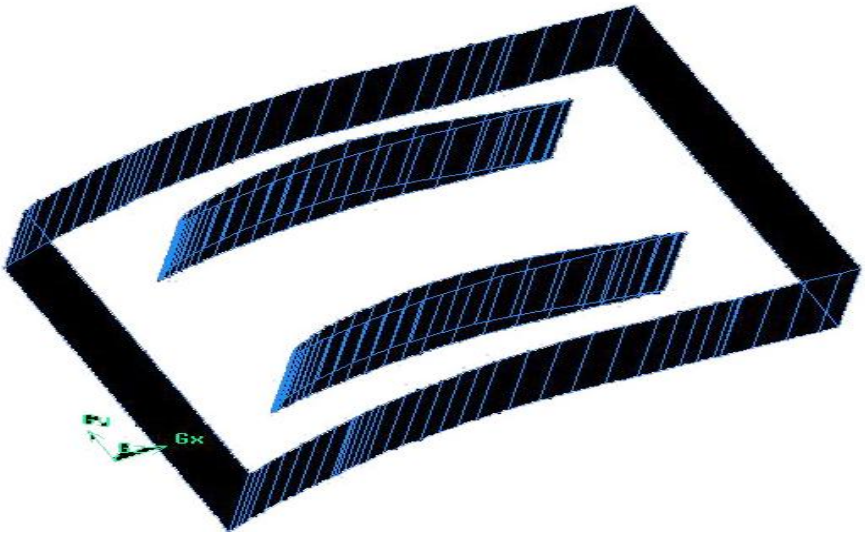

Figure 3: Gambit model of cascade blades with fluid volume (model 1)

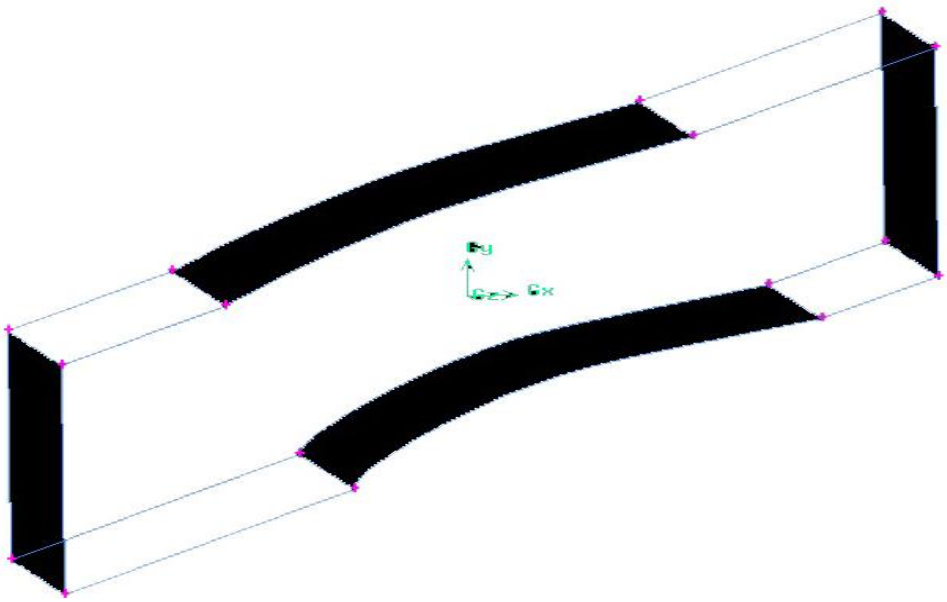

Figure 4: Volume of main flow under consideration (model 2)

This flow is cut out of the main flow stream under consideration from model 1.Sinc it is hard to numerically calculate for such a bid domain (model 1) in gambit and fluent both.

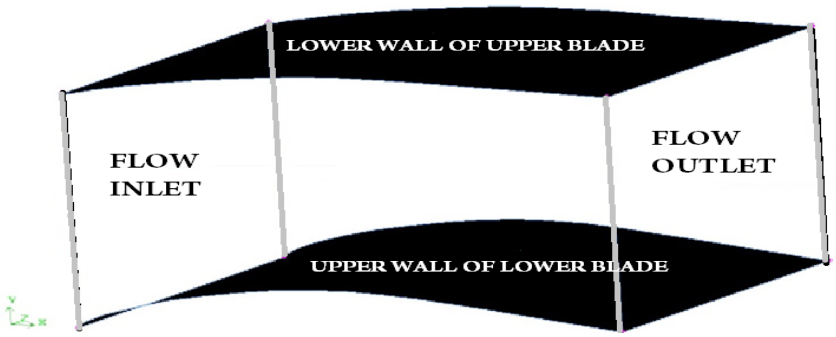

Figure 5: Flow volume between the blades only (model 3)

This figure is again the area between the blades only where we have to check the formation of the secondary flow vortex.

Meshing

Different types of mesh sizes, types, elements are available for edge, face and volume meshing. It must be the optimum size of mesh for getting the accurate results. Gambit software provides a wide range of meshing options for simple as well as complex geometries.

Table 2 Meshing details

1	Elements used for face meshing	Quadrilateral
2	Elements used for volume meshing	Tet/Hyd. & Quad/Tri
3	Interval count	According to length of edge
4	Side	Single sided
5	Successive ratio	1
6	Nodes	33201 (for model 3)

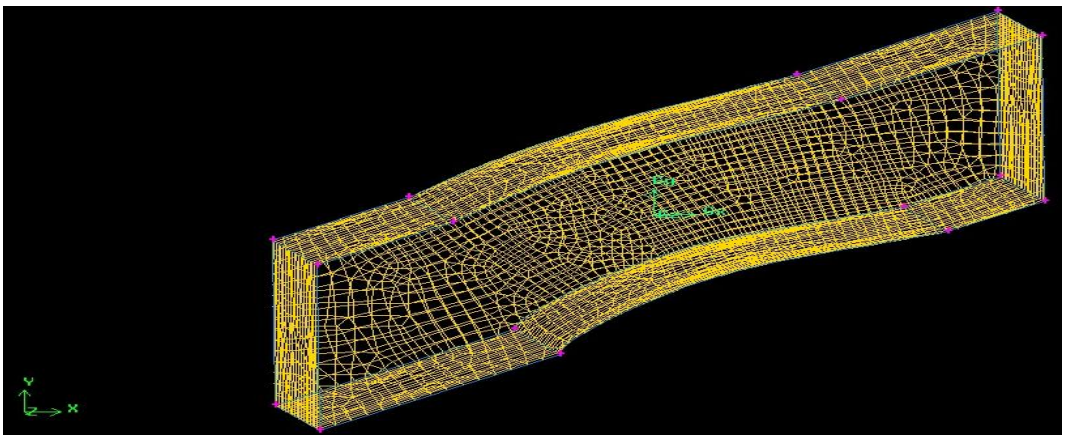

Figure 6: Meshing of model 2

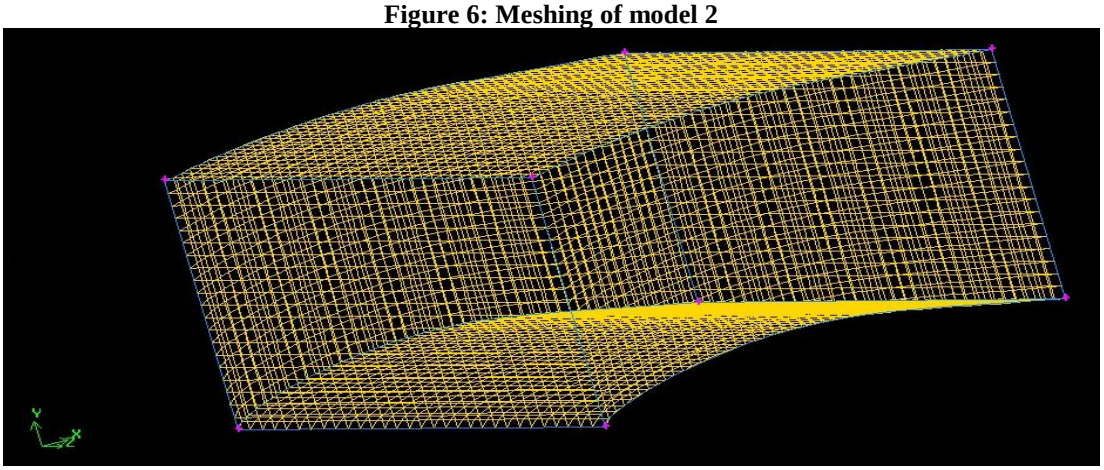

Figure 7: Meshing of model 3

Boundary conditions

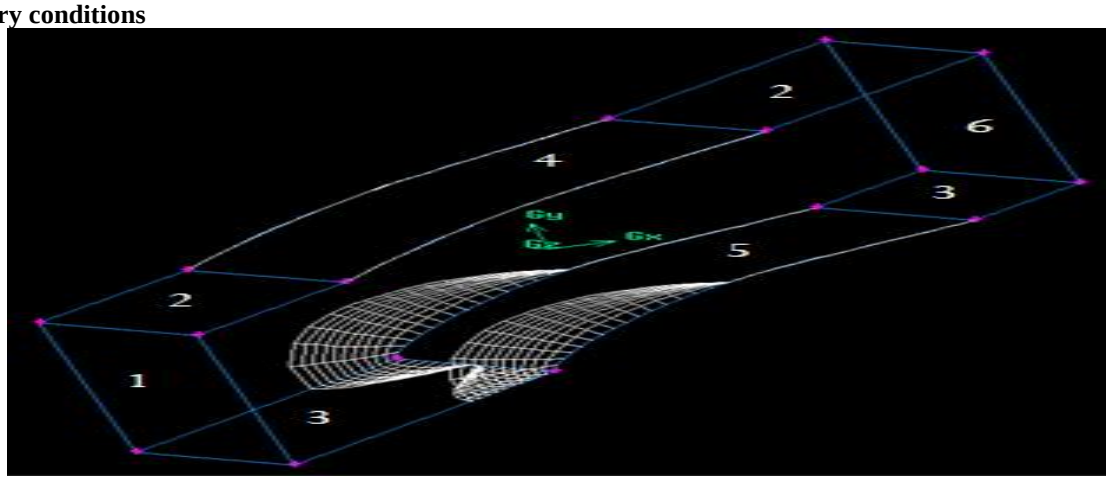

Figure 8: Different faces of model 2

Table 3 Boundary conditions

Face	Name	Boundary Condition
1	Inlet	Velocity
2,3	Side walls	Periodic \Wall
4	Suction side	Wall
5	Pressure side	Wall
6	Outlet	Pressure

Turbulence modelling

Turbulence Modelling, as turbulence affects the flow behaviour of the turbo machines, its consideration is critical in compressor blade analysis. The turbulence level seems to play a role on both the mixing within, and between the structures. Compressor blade model use k-epsilon turbulence model with realizable option. The k-epsilon model is mainly used for confined flows which usually occurred in turbo machines blade cascades and for high Reynolds number flows such as this problem. The realizable K-epsilon model gives more accurate results than any other turbulence model for the annular cascade. It also correctly predicts the boundary layer flows near the tip wall region in the cascade.

Table 4 Solution Controls for turbulence Modelling

Under relaxation factors	**Values**
Turbulent Kinetic Energy	0.8
Turbulent Dissipation Energy	0.8
Turbulent Viscosity	1
Discretization	**Order**
Flow	Second order upwind
Turbulent Kinetic Energy	Second order upwind
Turbulent Dissipation Rate	Second order upwind

Results and discussion

In order to recognize the secondary flow formation between the two blades of compressor cascade, a numerical simulation using CFD method is performed for axial flow compressor cascade. Input conditions are provided in the form of boundary conditions for velocity inlet at inlet face the velocity was set to 250 m/s that is approx. equal to Ma = 0.66. The α_i is varied as 26.5^o (for model 2 only), 35^o and 45^o (for model 3). Their intensity is shown to be strongly dependent on the inlet flow angle.

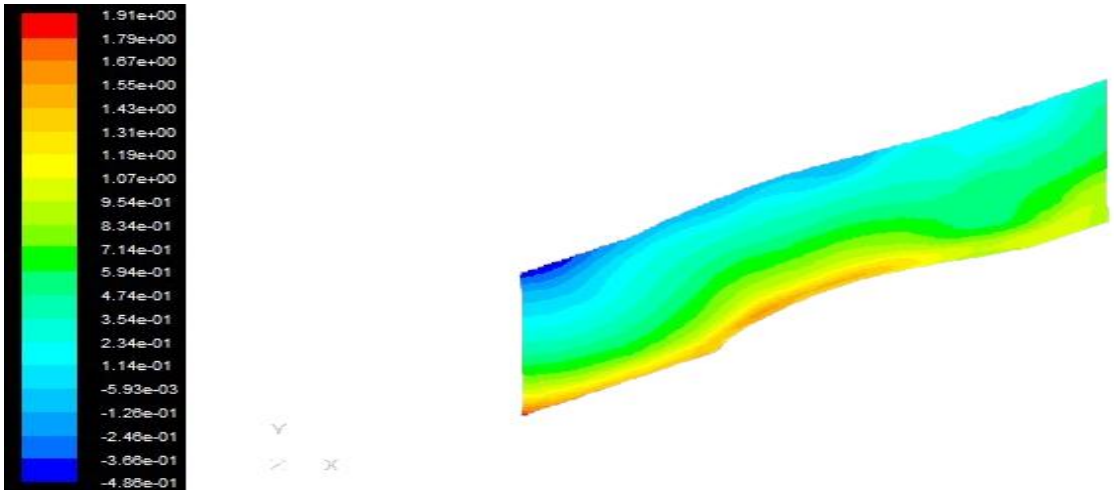

Figure 9: Contours of total pressure for model 2.

In figure 9 we can see the contours of total pressure which is showing a slight increase in the inlet pressure. This is the condition for inclination of 26.5 degree angle. But in this geometry we cannot see the flow behaviour near the blades. So there is a need of geometry of third type.

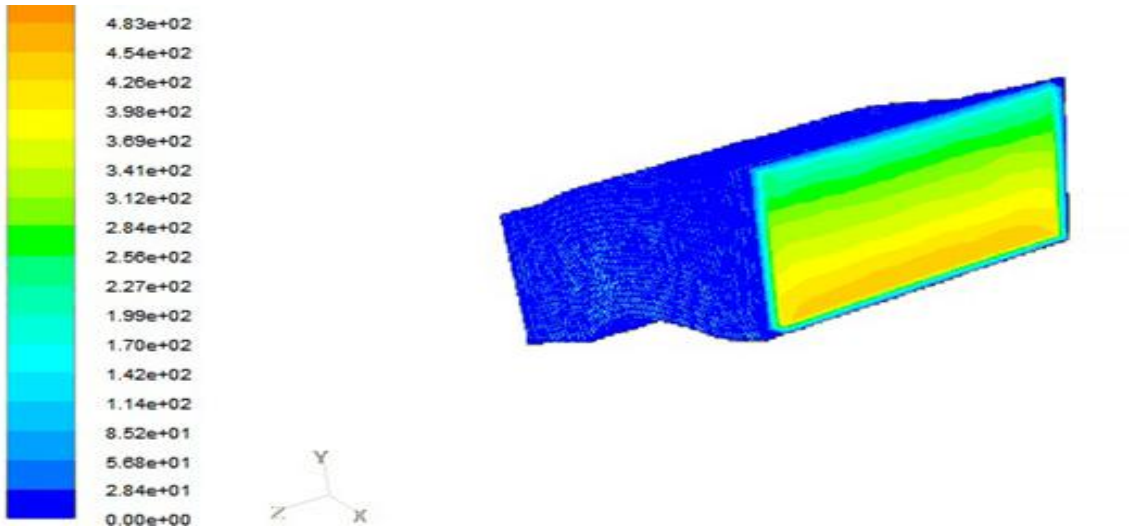

Figure 10: Contours of velocity magnitude for model 2.

Figure 10 tells about the contours of velocity magnitude at the outlet of the flow of model 2. The dark area shows the stagnation of the flow particles next to the wall.

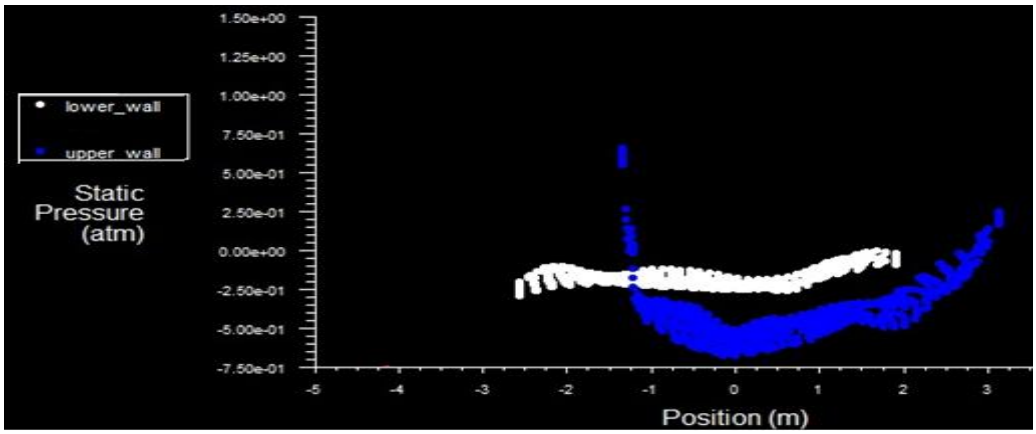

Figure 11: Static pressure for pressure side and suction side for model 2

This figure shows the gauge pressure variation along the length of the blades both in the lower wall that is pressure side and upper wall that is suction side. A little increase in pressure can be seen in both the walls here.

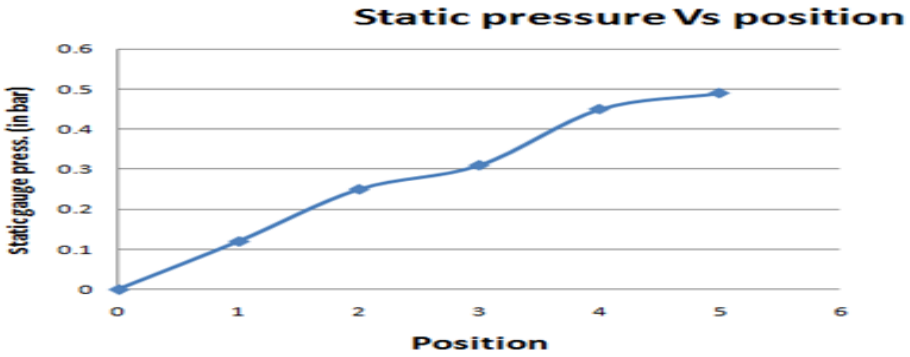

Figure 12: Variation of static pressure with the position in model 2 at 0^o incidence

This plot gives the variation of static pressure for the zero degree incident angle. In this we can see that the compressor cascade is giving the rise in the pressure from leading edge to trailing edge.

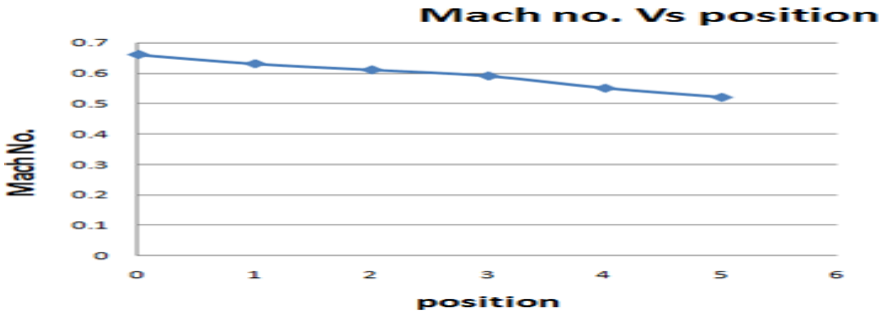

Figure 13: Variation of Ma with the position in model 2 at 0^o incidence

The inlet Mach number taken here is 0.66 but due to the decrease in velocity throughout the cascade flow there is a decrease in Ma can be seen. The outlet Mach number comes around 0.52. All the values taken for plotting these graphs are averaged and approximate.

Model 3 represents the volume of fluid flow between the two blades only. This model consists of 33201 nodes and is not showing behaviour of compressor cascades at high incidence angles since with high incidence angles they act more like a turbine cascade. Here number of iterations done is 500.

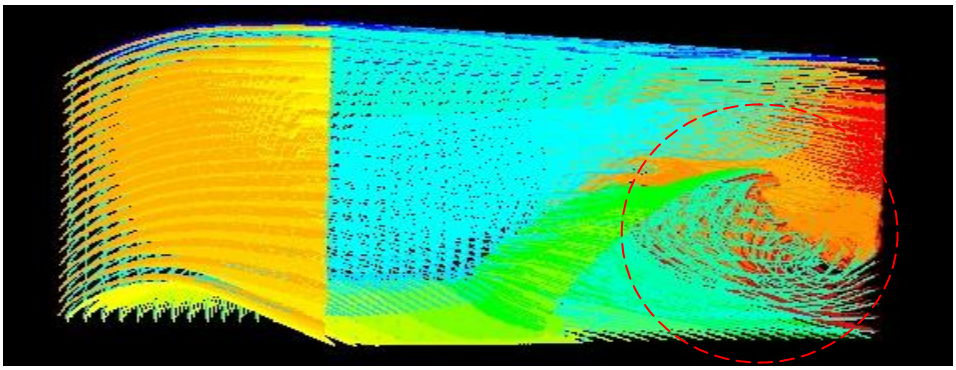

Figure 14: Path lines of flow in model 3

Here the path lines of the fluid flow inside the volume taken under consideration at 35^o. The bottom side encircled of upper wall of first blade is showing a vortex kind of structure coming out from the cascade which confirms the formation of secondary flow.

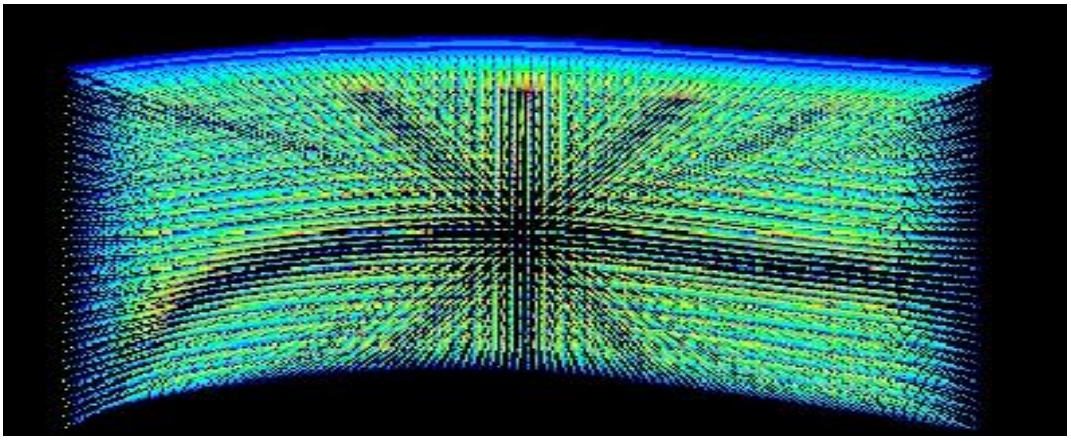

Figure 15: Path lines showing only lower wall and interior flow

This figure is also showing the path lines with respect to the lower wall of second or upper blade only. In that also a main vortex stream can be seen from inlet to outlet of the internal flow through the volume that confirms the formation of passage vortex.

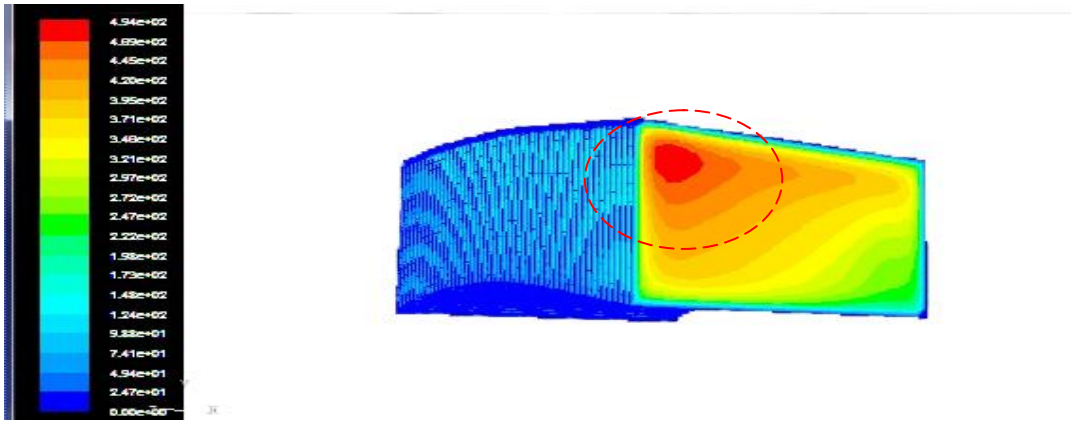

Figure 16: Contours of velocity magnitude (m/s) at outlet for model 3

The above figure shows the counters of velocity at outlet 45^{o} inlet of air. The outside face can be seen here that shows encircled area were the velocity of the air is high. This is confirming the vortex kind of flow taking place at that area in between the blades.

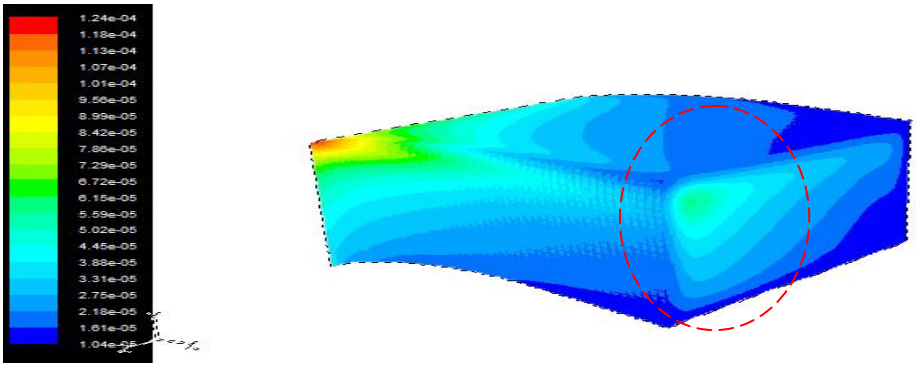

Figure 17: Contours of total pressure (atm) for model 3

This figure also shows the vortex of high pressure region in the outlet face at 45^{o}. So vortex kind of flow exists inside the blade flow volume. The cascade gives us a small pressure rise at most of the place approximately about 0.5 times. The graphs shown below are showing the change in properties of flow while moving from leading edge to trailing edge.

Conclusions

1. By this analysis we can conclude that in axial flow compressors the threat of secondary loss is less because it suffers low inlet angle where secondary flow is hardly formed.
2. In compressors secondary flow effects are less because of less turning or bending while passing through blade passage.
3. Secondary flow effects can be seen in the axial flow compressor with high incidence angles like 35 or 45 degrees.

Appendix (Blade Coordinates)

Suction	Suction	Pressure	Pressure	Mean
5.001	0.000	5.001	0.000	0.000
4.902	0.020	4.901	0.009	0.015
4.703	0.061	4.699	0.028	0.044
4.404	0.119	4.497	0.046	0.083
4.257	0.148	4.245	0.069	0.108
4.010	0.202	3.992	0.092	0.147
3.612	0.285	3.590	0.132	0.208
3.213	0.359	3.189	0.169	0.264
2.811	0.420	2.790	0.198	0.309
2.404	0.456	2.397	0.213	0.335
1.997	0.460	2.004	0.210	0.335
1.744	0.448	1.575	0.201	0.325
1.491	0.427	1.510	0.189	0.308
1.238	0.396	1.263	0.172	0.284
0.986	0.356	1.015	0.150	0.254
0.734	0.304	0.766	0.122	0.213
0.483	0.239	0.517	0.087	0.163
0.383	0.209	0.417	0.071	0.140
0.283	0.174	0.317	0.053	0.114
0.184	0.134	0.216	0.034	0.084
0.086	0.084	0.114	0.013	0.049
0.038	0.053	0.062	0.002	0.028
0.016	0.033	0.340	-0.002	0.015
0.000	0.011	0.010	-0.004	0.004
0.000	0.000	0.000	0.000	0.000

References

1. **A. Hergt, R. Meyer and K. Engel**, Experimental and numerical investigation of secondary flow on compressor blades
2. **Krishna Nandan Kumar** and **M. Govardhan,** 2010, Secondary Flow Loss Reduction in a Turbine Cascade with a Linearly Varied Height Stream wise End wall Fence. *Hindawi Publishing Corporation, International Journal of Rotating machinery, Volume 2011, Article ID 352819*
3. **Hyon Koon Myong** & **Seung Yong Yang,** the numerical investigation for getting flow characteristics at blade passage tip clearance in a linear cascade of high performance turbine blade'. *KSME International Journal Vol.17 no. 4 page 606-616,2003*

4. **Nikolay Ivanov, Valery Goriatchev, Evgueni Smirnov and Vladimir RIS**, 'CFD analysis of secondary flow and pressure losses in a NASA Transonic turbine cascade.' *Conference of modelling fluid flow, Hungary September 2003*.
5. **J. Dunham** 'A review of cascade data on secondary losses in turbines'.
6. **J.H. Horlock, J.D. Denton** 'A review of some early design practise using Computational fluid dynamics and a current perspective.' *Cambridge University Engineering Department.*
7. **A. R. Howell, M.A.** 'Flow Dynamics of Axial Compressors.'
8. **Johan Hjarne, Valery Chernoray, Jonas Larsson, Lennart Lofdahl** 'An Experimental Investigation of secondary flows and loss development downstream of a highly loaded low pressure turbine outlet guide vane cascade.' *Asme Turbo Expo 2006*.
9. **Piotr Lampart, '**Investigation of end wall flows and losses in axial turbines. Part i. formation of end wall flows and losses.' *Journal of theoretical and applied mechanic 47, 2, pp. 321-342, Warsaw 2009*
10. **Anderson, J. D.** Jr., 1995: *Computational Fluid Dynamics, The Basics With Applications*, *McGraw-Hill Inc., Singapore.*
11. **B. Lakshminarayan & J.H. Horlock** , Text book of turbomachinery
12. **Yahya S.M.** 1998, *Turbines, Compressors and Fans*, Tata Mc-Graw-hill publishing company limited.
13. **Dixon S.L.** 1998, *Fluid mechanics and thermodynamics of turbo machines*, Reed Educational and Professional Publishing Ltd.
14. **Ghoshdastidar P**, *Computer simulation of flow and heat transfer* , TMH New Delhi publication
15. **Fluent,** (1998) FLUENT 6 User´s Manual, *Fluent. Inc*
16. **Gambit** user's manuals.